


Article

# Desulfurization Performance of Choline Chloride-Based Deep Eutectic Solvents in the Presence of Graphene Oxide

Chiau Yuan Lim <sup>1</sup>, Mohd Faridzuan Majid <sup>1</sup>, Sarrthesvaarni Rajasuriyan <sup>1</sup>,  
Hayyiratul Fatimah Mohd Zaid <sup>1,2,\*</sup>, Khairulazhar Jumbri <sup>1,3</sup> and Fai Kait Chong <sup>1</sup>

<sup>1</sup> Department of Fundamental and Applied Science, Universiti Teknologi Petronas, Tronoh, Perak 31750, Malaysia; Lcy6786@hotmail.com (C.Y.L.); m.faridzuan.majid@gmail.com (M.F.M.); vaarnisarthes@gmail.com (S.R.); khairulazhar.jumbri@utp.edu.my (K.J.); chongfaikait@utp.edu.my (F.K.C.)

<sup>2</sup> Centre of Innovative Nanostructures & Nanodevices (COINN), Universiti Teknologi Petronas, Tronoh, Perak 31750, Malaysia

<sup>3</sup> Centre for Research in Ionic Liquids (CORIL), Universiti Teknologi Petronas, Tronoh, Perak 31750, Malaysia

\* Correspondence: hayyiratul.mzaid@utp.edu.my; Tel.: +605-368-7618

Received: 23 September 2020; Accepted: 30 October 2020; Published: 2 November 2020



**Abstract:** Extractive catalytic oxidative desulfurization (ECODS) is the one of the recent methods used in fuel desulfurization which involved the use of catalyst in the oxidative desulfurization of diesel fuel. This study is aimed to test the effectiveness of synthesized choline chloride (ChCl) based deep eutectic solvent (DES) in fuel desulfurization via ECODS method, with the presence of graphene oxide (GO) as catalyst and hydrogen peroxide (H<sub>2</sub>O<sub>2</sub>) as oxidant. In this study, 16 DESs based on choline chloride were synthesized using glycerol (GLY), ethylene glycol (EG), tetraethylene glycol (TEG) and polyethylene glycol (PEG). The characterization of the synthesized DES was carried out via Fourier transform infrared spectroscopy (FTIR) analysis, density, and viscosity determination. According to the screening result, ChCl-PEG (1:4) was found to be the most effective DES for desulfurization using ECODS method, with a removal of up to 47.4% of sulfur containing compounds in model oil in just 10 min per cycle after the optimization of the reaction parameters, and up to 95% desulfurization efficiency could be achieved by six cycles of desulfurization. It is found that the addition of GO as catalyst does not increase the desulfurization performance drastically; hence, future studies for the desulfurization performance of DESs made up from ChCl and PEG and its derivatives can be done simply by using extraction desulfurization (EDS) method instead of ECODS method, for cost reduction purpose and easier regulation of DES waste into environment.

**Keywords:** deep eutectic solvent; desulfurization; graphene oxide

## 1. Introduction

Sulfur containing compounds (SCC) are usually present in diesel fuel, which is commonly used in heavy type of vehicle or machines as a source of energy. There are a few examples of SCC in diesel fuel such as thiols, sulfides, disulfides, thiophenes, benzothiophenes (BT), and dibenzothiophenes (DBT) [1]. The combustion of diesel fuels leads to the formation of sulfur dioxide (SO<sub>2</sub>) and its derivatives which are then released into the atmosphere. SO<sub>2</sub> is known for causing air pollution, acid rain and irritation to human skin, eyes, nose, throat, and lungs. Previous research reports that the deposition of acidic sulfur (from acid rain) into the forest soil can cause the releasing of methane gas, which is one of the greenhouse gases into the atmosphere [2]. The remnant of sulfur in diesel fuel also reduces the effectiveness of catalyst used in the emission control system which is crucial in oxidation of the carbon monoxide and hydrocarbon into relatively harmless carbon dioxide before emitting the gases into the

surrounding atmosphere. In order to regulate the toxic gas emission from diesel fuel, the government proposed a more stringent environmental regulation to control the SCC concentration in diesel fuel to be less than 10 ppm [3,4].

Hydrodesulfurization (HDS) method is still being used as the commercial method for fuel desulfurization. With the presence of expensive catalyst such as Co-Mo/Al<sub>2</sub>O<sub>3</sub> or Ni-Mo/Al<sub>2</sub>O<sub>3</sub> and extreme reaction condition such as high temperature (300–340 °C) and high pressure (20–100 atm of hydrogen gas), SCC reacts with the hydrogen gas to form hydrogen sulfide gas, which is later removed from the diesel fuel as elemental sulfur or sulfuric acid [5]. The high cost of maintenance fee and the inability to remove sterically hindered SCC such as alkyl-substituted BT and DBT are often the major drawbacks of the HDS method.

A wide range of desulfurization methods, namely biodesulfurization (BDS), extractive desulfurization (EDS), oxidative desulfurization (ODS), and adsorption desulfurization (ADS) have been proposed by researchers in order to enhance fuel desulfurization performance. The BDS method involves the use of microorganisms such as bacteria to remove the SCC from diesel fuel [6]. The advantage of utilizing BDS method includes having low cost and is environmentally friendly as it does not produce toxic gases or greenhouse gases during the desulfurization process. However, the drawbacks of BDS method are that it requires long operational duration and the need to maintain the specific living condition for the bacteria to work optimally, by using a chemostat [7] or a fermenter [8], increasing the operational cost.

While for ADS, the removal of sulfur from diesel fuel can be done via passive adsorption by an adsorbent. Examples of adsorbents are zinc oxide, zeolites, alumina, aluminosilicates, and activated carbon. There are reports that prove that ADS demonstrate good desulfurization performance, especially for the 4,6-dimethyldibenzothiophene, which is a sterically hindered SCC [9,10]. However, the constant regeneration of the used adsorbent is a limiting step for this method.

EDS method involves the use of a solvent to selectively remove SCC from fuels through liquid-liquid extraction. The extraction solvents can be organic solvents, ionic liquid (IL), or deep eutectic solvent (DES), as long as there is a difference in polarity with the diesel fuel [1]. Many researchers have used this approach to test the desulfurization performance of their synthesized IL or DES due to its simplicity [11,12].

The ODS method involves catalytic oxidation of the SCC in the fuel to their analogical sulfoxide or sulfones. H<sub>2</sub>O<sub>2</sub> is often chosen as the oxidant in ODS as it does not produce harmful by-products. The oxidized SCC having increased polarity and molecular weight, is easier to be extracted from diesel fuel via extraction or adsorption using appropriate extraction solvent or solid adsorbent [13,14]. However, the waste produced from the oxidation of SCC need to be properly managed as it is hazardous to the environment.

In this study, the authors integrate the EDS and ODS method, with the addition of catalyst as to further improve the fuel desulfurization process. Previous researchers have reported that the use of hydroperoxides as oxidants, in combination with in situ produced per-acid or catalyst is able to provide deep desulfurization on diesel fuel [15]. Common catalyst used in the extractive catalytic oxidative desulfurization (ECODS) method are photocatalysts and nanocomposites [16,17]. In this study, the author has chosen graphene oxide (GO) as the catalyst as it is widely used in catalytic processes. The advantage of using carbon-based catalyst is that it is cheaper, chemically inert to the reactant, and can be easily regenerated. Several researchers report that graphene oxide is very helpful in improving the functionality of fuel cell [13], removing nitro compound during the waste water treatment [18], and in fuel desulfurization [19].

Deep eutectic solvent (DES) is a eutectic mixture that is made up of two or more components, involving the electrostatic force and  $\pi$ - $\pi$  interaction between a hydrogen bond acceptor (HBA) and a hydrogen bond donor (HBD) [20]. Synthesized DES would generally have lower melting point than their individual components [21]. Recently, researchers have shown growing interests towards the usage of DES, as compared to ILs. There are a few reasons for the DES to be chosen over IL for the

current fuel desulfurization research. Firstly, the cost of synthesizing DES is much lower than IL, as the starting materials for DES are relatively cheaper and widely available in the laboratory [22]. Some of the IL involves the use of organic solvents as one of their starting material, and environmental problem might arise if the IL waste is not properly managed, as compared to DES, which are considered biodegradable [23,24]. DES has the ability to function as a “designer solvent”, where researchers can tailor make the DES according to the requirement of the processes involved in their study [25]. DES are also immiscible in non-polar solvents typically diesel fuel making the regeneration of DES easier which is somehow favorable in petroleum refinery [26].

Generally, there are four types of DES, namely type I, type II, type III, and type IV. Type I to type III DES solvents are made up by mixing quaternary salts and metal halide (Type I), hydrated metal halide (Type II) and HBD (Type III). Type IV DES involves the mixing between metal halide and HBD. In this study, type III DES solvent is utilized, thus we will use the quaternary salt as HBA. There are some examples of HBA such as ChCl, Tetrabutylammonium bromide (TBAB), Tetrabutylammonium chloride (TBAC), Methylimidazole, Dimethylamine and L-proline. Generally, HBD are made up of glycerol, glycol, acid, amide, and alcohol groups, which readily donate their free hydrogen to HBA. DESs based on choline chloride (ChCl) have been shown to be effective for fuel desulfurization study [25]. However, the hygroscopic nature of ChCl is known to have an effect on the desulfurization performance for the ChCl-based DES; hence, during the preparation stage, it is very important to always dry the ChCl salt prior to usage in DES.

In this study, 16 different DESs were prepared by mixing ChCl with four different types of HBDs, namely glycerol, ethylene glycol, tetraethylene glycol, and polyethylene glycol in molar ratios ranging from 1:1 to 1:4. The physiochemical properties of the synthesized DES, including the density and viscosity were measured. It is proven that DES with high density and viscosity would affect their desulfurization performance [27,28]. FTIR analysis was also carried out to characterize and compare the four different types of ChCl-based DES based on their functional groups. After the screening process, the selected DES underwent several experiments to find the optimal reaction conditions. Lastly, the desulfurization performance by selected DES on real diesel fuel was evaluated.

## 2. Experimental Method

### 2.1. Chemicals

Choline chloride (ChCl, 99.0%), glycerol (GLY), ethylene glycol (EG, 99.5%), tetraethylene glycol (TEG, 98.0%), and polyethylene glycol 400 (PEG 400) were purchased from SigmaAlrich (St. Louis, Missouri, USA). Dibenzothiophene (DBT, 99.0%), *n*-dodecane (99.0%), hydrogen peroxide (H<sub>2</sub>O<sub>2</sub>), and reduced GO were purchased from Merck (Kenilworth, New Jersey, USA).

### 2.2. DES Preparation

The DESs were prepared by mixing ChCl with GLY, EG, TEG, and PEG in molar ratios ranging from 1:1 to 1:4. ChCl acted as a HBA, while GLY, EG, TEG, and PEG served as HBDs. ChCl was dried in an oven overnight at 80 °C due to its hygroscopic nature. The HBA and HBD were mixed in the desired molar ratio in a vial and stirred at either 60 or 80 °C until a homogenous solution was obtained. DES preparation conditions are summarized in Table 1.

**Table 1.** Deep eutectic solvent (DES) preparation conditions.

DES	Temperature (°C)	Stirring Speed (rpm)	Time (min)
ChCl-GLY	60	500	60
ChCl-EG			
ChCl-TEG			
ChCl-PEG	80	500	90

### 2.3. Density and Viscosity

The density and viscosity of each DES were measured at temperatures ranging from 25 to 90 °C using a SVM 3000 viscometer (Anton Paar, Graz, Austria). The viscometer was first calibrated using a solution with a known density supplied by the manufacturer.

### 2.4. Fourier Transform Infrared Chromatography (FTIR)

Perkin Elmer FTIR spectrometer Frontier was used for the functional group characterization of the synthesized DESs. Background spectrum was collected prior to the procedure as to eliminate unwanted residual peak from the sample spectrum. The wavenumbers produced by the DESs and their pure components were recorded from 400 to 4000  $\text{cm}^{-1}$ .

### 2.5. Extractive Catalytic Oxidative Desulfurization Process

The performance of the DESs for ECODS was evaluated using  $\text{H}_2\text{O}_2$  as an oxidant and GO as the catalyst. The *n*-dodecane was used to prepare model oil (MO) that contained 100 ppm dibenzothiophene (DBT) as the SCC. Each DES was mixed with the MO at a 1:5 (*v/v*) ratio in a reaction vial. The molar ratio of oxygen to sulfur (O/S) in each mixture was 6:1, and the GO/S mass ratio was set at 1:25. The reaction mixtures were stirred at 400 rpm for one hour at room temperature (~25 °C), after which the contents were allowed to settle for 30 min. Approximately 2 mL was removed from the upper layer of each reaction mixture for HPLC analysis to find out the DBT concentration in the MO. The HPLC instrumental details and parameters are shown in Table 2.

**Table 2.** HPLC instrumentation and parameters.

Equipment Model	HPLC Agilent 1200 Infinity Series
Columns	Reversed-phase ZORBAX SB-C18 (4.6 × 150 mm)
Detector	Ultraviolet-visible detector
Mobile phase	Methanol: water: isopropanol (90:8:2) with flow rate of 1 mL min <sup>-1</sup>
Injection volume	1 μL
Detection wavelength	310 nm

### 2.6. Extractive Catalytic Oxidative Desulfurization Parameters

The DES with the best desulfurization performance was further used in the optimization process in order to determine the optimal reaction conditions for the fuel desulfurization to occur via ECODS method.

#### 2.6.1. Volume Ratio of DES to the Model Oil

The volume ratio of DES to MO was set at 2.5:1, 1:1, 1:2.5, 1:5, and 1:10, respectively, as the manipulated variables for this experiment. The DES/MO volume ratio of 2.5:1 and 1:1 were served as control of the experiment to prove directly whether the selected DES has the potential to perform well in fuel desulfurization. In this experiment, the mass ratio of GO/S was set as 1:25 and molar ratio of  $\text{H}_2\text{O}_2/\text{S}$  was set as 6:1. The reaction mixture was filled into a reaction vial with a magnetic stirrer by pipetting the individual components using a micropipette accordingly. The reaction mixture was then stirred at 400 rpm for one hour under room temperature. After one hour of stirring, the reaction mixture was left aside for 30 min, in order to let the DES layer to settle at bottom of the reaction vial. Then, approximately 2 mL of the upper layer of the reaction mixture (model oil layer) was carefully syringed out using a micropipette and stored in a labelled HPLC vial. The experiment procedure was repeated for another two times to obtain more reliable result.

### 2.6.2. Effect of Oxidant Amount

The molar ratio of  $H_2O_2$  to S was set at 0, 2:1, 4:1, 6:1, and 8:1 as the manipulated variables for this experiment. In this experiment, the mass ratio of GO/S was set as 1:25 and volume ratio of DES to MO was set as 1:2.5. The reaction mixture was filled into a reaction vial with a magnetic stirrer by pipetting the individual components using a micropipette accordingly. The same steps were repeated as in the previous section.

### 2.6.3. Catalyst Dosage

The mass ratio of GO to sulfur (S) was set at 0, 1:400, 1:200, 1:100, 1:50, and 1:25 as the manipulated variables for this experiment. In this experiment, the molar ratio of  $H_2O_2$ /S was set as 4:1 and volume ratio of DES to MO was set as 1:2.5. The reaction mixture was filled into a reaction vial with a magnetic stirrer by pipetting the individual components using a micropipette accordingly. The same steps were repeated as in the previous section.

### 2.6.4. Effect of Temperature

The reaction temperature was set at 25, 40, 50 and 60 °C as the manipulated variables for this experiment. In this experiment, the molar ratio of  $H_2O_2$  to S was set as 4:1, the mass ratio of GO/S was set as 1:100 and volume ratio of DES to MO was set as 1:2.5. The same steps were repeated as in the previous section.

### 2.6.5. Effect of Stirring Speed

The stirring speed was set as 200, 400, 600, 800 and 1000 rpm as the manipulated variables for this experiment. In this experiment, the molar ratio of  $H_2O_2$  to S was set as 4:1, the mass ratio of GO/S was set as 1:100 and volume ratio of DES to MO was set as 1:2.5. The same steps were repeated as in the previous section.

### 2.6.6. Effect of Reaction Time

The reaction time was firstly set at 5 min, followed by 10 min, after that every 10-min interval from 20 min to 1 h, and later, every one-hour interval from 1 h to 8 h. In this experiment, the molar ratio of  $H_2O_2$  to S was set at 4:1, the mass ratio of GO/S was set as 1:100 and volume ratio of DES to MO was set as 1:2.5. The same steps were repeated as in the previous section.

### 2.6.7. Multistage Extraction

In this experiment, the optimal reaction parameter for the selected DES was utilized. The molar ratio of  $H_2O_2$  to S was set at 4:1, the mass ratio of GO/S was set as 1:100, volume ratio of DES to MO was set as 1:2.5, reaction temperature was set as 25 °C, stirring speed was set at 400 rpm, and the reaction time was set at 10 min for every stage of the catalytic oxidative desulfurization process. In the first stage, 45 mL of model oil was filled into a reaction vial with a magnetic stirrer by pipetting the individual components using a micropipette accordingly. The reaction mixture was then stirred at 400 rpm for 10 min under room temperature. After that, the reaction mixture was left aside for 30 min, in order to let the DES layer to settle at bottom of the reaction vial. Then, approximately 2 mL of the upper layer of the reaction mixture (model oil layer) was carefully syringed out using micropipette and stored in a labelled HPLC vial. In the second stage, 40 mL of the reacted model oil from the first stage was pipetted to a new reaction vial, followed with the respective DES/MO volume ratio, molar ratio of  $H_2O_2$ /S, and mass ratio of GO/S. The same steps was taken as in the first stage. The experimental procedure was repeated for third stage by using 35 mL leftover reacted model oil from the second desulfurization stage, fourth stage by using 30 mL, fifth stage by using 25 mL, and finally the sixth stage by using 20 mL leftover reacted model oil. The experiment procedure was repeated for another two times to obtain more reliable result.

### 2.6.8. Desulfurization in Real Diesel Fuel

Real diesel fuel was collected from Petronas fuel station in Tronoh, Iskandar. The experimental procedure was similar to Section 2.6.7, where the real diesel fuel underwent six stage of catalytic oxidative desulfurization with the selected DES. This was carried out to test the ability of the selected DES to be applied in industrial petroleum refinery.

## 3. Result and Discussion

### 3.1. DES Preparation

Four different types of DES, namely Choline Chloride-Glycerol (ChCl-GLY), Choline Chloride-Ethylene Glycol (ChCl-EG), Choline Chloride-Tetraethylene Glycol (ChCl-TEG), and Choline Chloride-Polyethylene Glycol (ChCl-PEG) were successfully prepared with mol ratio of HBA:HBD from 1:1 to 1:4. Table 3 describes the physical appearance of each of the prepared DES. Based on previous literatures, only the DES that are able to form a clear transparent liquid is chosen for the characterization [28–30]. However, in this work, all the DES were characterized using FTIR and physical properties that include density and viscosity of the prepared DESs. Figure 1 illustrates the chemical interaction between the HBA and HBD during the preparation of DES. Electrostatic force is found between the positively charged nitrogen centre of the choline and negatively charged chloride ion in the ChCl salt. From the definition, it is known that DES is formed from a HBD and a HBA. According to Figure 1, hydrogen bond between the DES is formed between the hydrogen of the hydroxyl group from the HBD with the chloride ion from the ChCl salt which acts as HBA.

**Table 3.** Physical description of synthesized DES under room temperature.

DES	Mole Ratio	Physical Appearance
ChCl-GLY	1:1	Highly viscous liquid
	1:2	Transparent viscous liquid
	1:3	Clear transparent liquid
	1:4	Clear transparent liquid
ChCl-EG	1:1	Transparent liquid with white precipitate
	1:2	Clear transparent liquid
	1:3	Clear transparent liquid
	1:4	Clear transparent liquid
ChCl-TEG	1:1	Highly viscous liquid
	1:2	Transparent liquid with white precipitate
	1:3	Clear transparent liquid
	1:4	Clear transparent liquid
ChCl-PEG	1:1	White sticky semisolid
	1:2	White sticky semisolid
	1:3	Highly viscous liquid
	1:4	Clear transparent liquid

### 3.2. Density and Viscosity

The density and viscosity are two most important physiochemical properties that can affect the effectiveness of DES on fuel desulfurization. Generally, the densities and viscosities of the DESs prepared in this study decreased with increasing temperature. As seen in Figure 2, the density of the prepared DESs decreased following the order ChCl-GLY (1:4) > ChCl-GLY (1:3) > ChCl-EG (1:2) > ChCl-EG (1:3) > ChCl-EG (1:4) > ChCl-TEG (1:3) > ChCl-TEG (1:4) ≈ ChCl-PEG (1:4). ChCl-EG, ChCl-TEG and ChCl-PEG had similar densities; however, their densities were found to decrease as the number of ethylene groups and the proportion of HBD in the DESs increased, similar observation as reported by Makoś and Boczka [29]. Oppositely, the densities of ChCl-GLY increased as the proportion of GLY decreased.



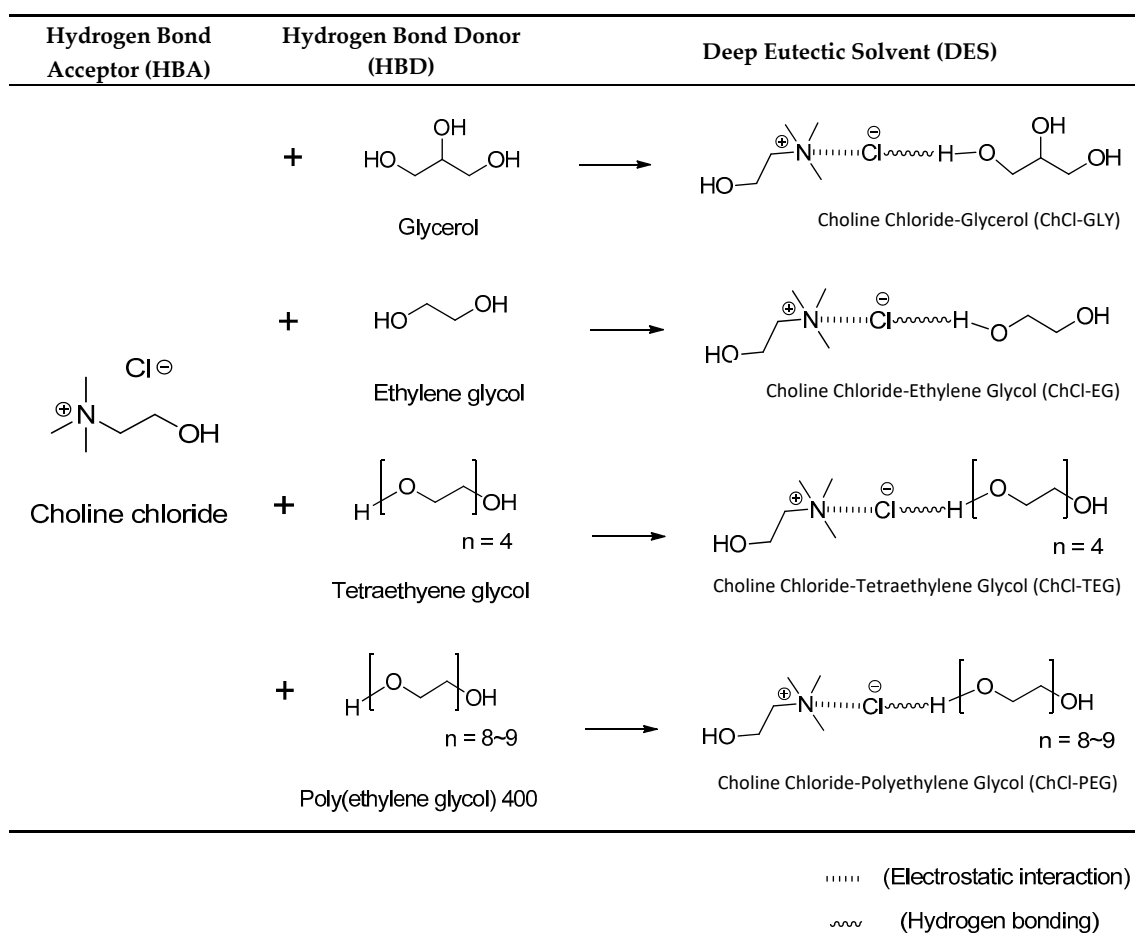


**Figure 1.** Reactions involved in the preparation of DES.

The viscosity value was determined as it is proven that there is a good correlation between fluidity and molar conductivity of the DES, whereby the fluidity can be calculated as reciprocal of viscosity [30]. Most of the DES synthesized was reported with viscosity value around 100 cP to 200 cP at room temperature, and the similar result are shown in Figure 3. According to Figure 3, the viscosity of the prepared DESs decreased in the order of ChCl-GLY (1:4) > ChCl-GLY (1:3) > ChCl-PEG (1:4) > ChCl-TEG (1:3) > ChCl-TEG (1:4) > ChCl-EG (1:2) > ChCl-EG (1:3) > ChCl-EG (1:4). High viscosity inhibits mass transfer as there might be presence of an extensive hydrogen-bonding network within the DES compounds itself which hinders the mobility of the free species available for fuel desulfurization process [31]. This may have been the reason why the performance of the highly viscous ChCl-GLY DESs was relatively poor in the desulfurization screening test. These results are discussed in Section 3.4.

### 3.3. Fourier Transform Infrared Chromatography

In the aspect of discovering new types of DES, FTIR is important in characterizing DES by predicting the functional group present in the DES. This is done by comparing the functional group found in the pure components as shown in Figure 4. The functional groups of a compound are usually illustrated as peaks in the FTIR graph, where each peak is caused by the vibration of the functional group due to the IR radiation from the FTIR machine. Different functional groups will show different values of absorbance or transmittance at slightly deviated wavenumbers based on their respective properties. By understanding the shifting of certain functional groups between pure compound and DES, it may help in the production of DES with more desirable properties in future studies. In this section, only the characterization of the four different types of DES in mol ratio of 1:4 will be discussed,

as the same type of DES will give out the same spectra as they have the same functional group and same bondings.

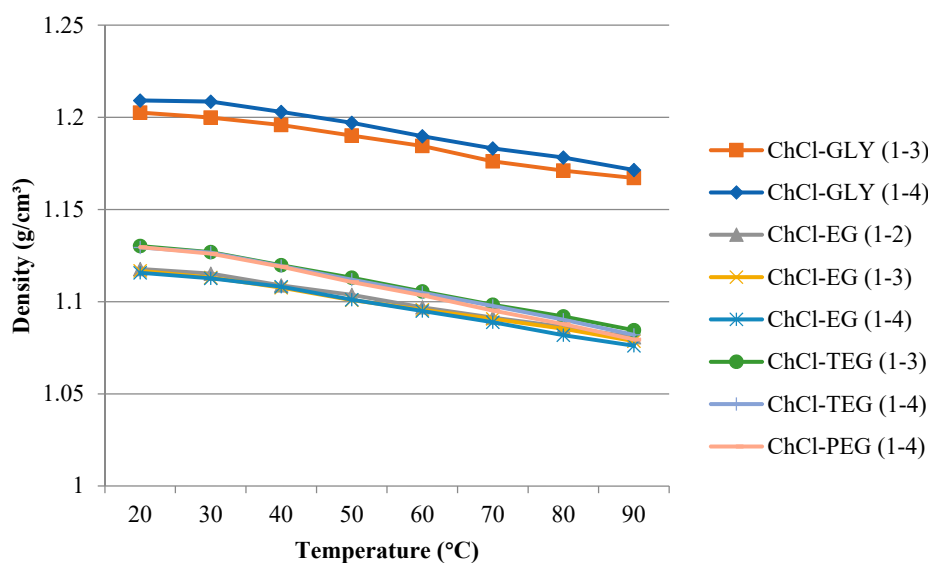


Figure 2. Density of DES with increasing temperature.

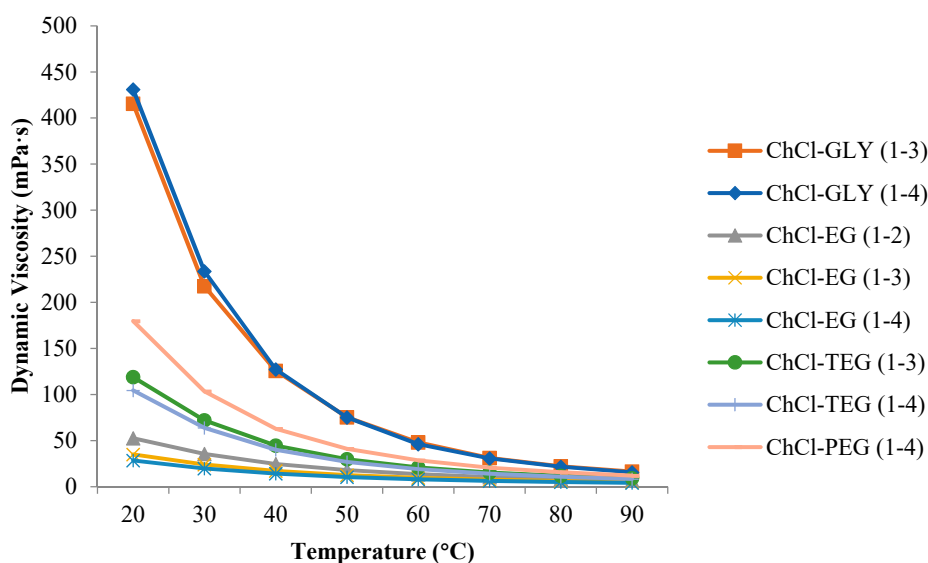


Figure 3. Changes in DES density with increasing temperature.

The stretching vibration of OH group was observed around  $3100\text{--}3700\text{ cm}^{-1}$ ; however, a previous study discovered that the OH peaks for glycol based deep eutectic solvent occurs around  $3200\text{--}3400\text{ cm}^{-1}$  [32]. The presence of OH group stretching vibration also indicates the presence of water content in the respective pure compound or prepared DES. According to Figure 4, glycerol (GLY) and ethylene glycol (EG) is found to have abroad peak around  $3281.52$  and  $3296.84\text{ cm}^{-1}$ , whereas the OH peak found in tetraethylene glycol (TEG) and polyethylene glycol (PEG) are less intense than that of GLY and EG, at around  $3409.11$  and  $3449.02\text{ cm}^{-1}$ , respectively. By comparing the four HBDs, the intensity of the OH peak is decreasing in the order of  $\text{GLY} > \text{EG} > \text{TEG} > \text{PEG}$ , suggesting that, the more aliphatic chain attached to the C-OH bond, the harder it will be for the compound to form hydrogen bonding with choline chloride.



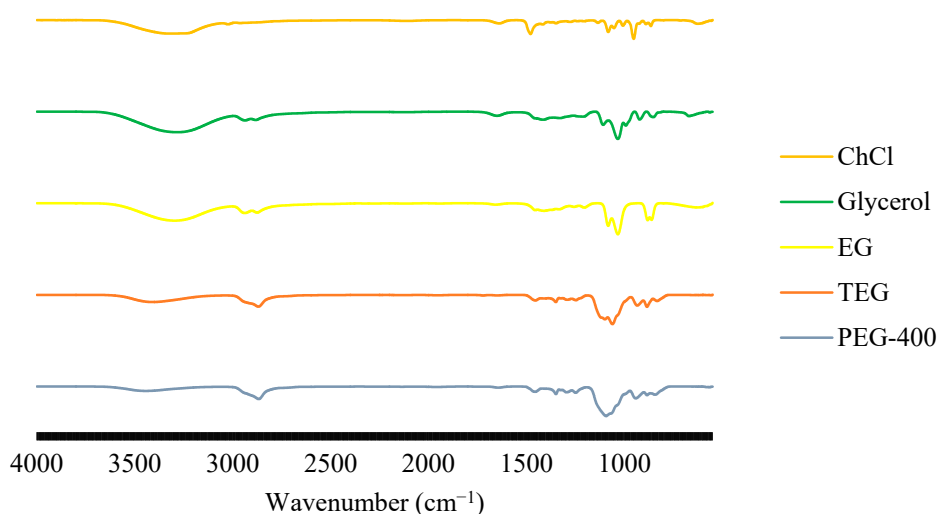


Figure 4. FTIR graph of the pure components.

In Figure 5, ChCl-GLY (1:4) has the most intense OH peak around  $3305.70\text{ cm}^{-1}$ , followed by ChCl-TEG (1:4), which has the OH peak around  $3307.67\text{ cm}^{-1}$ . The trend is followed by ChCl-TEG (1:4) which has moderate OH peak around  $3364.74\text{ cm}^{-1}$  and ChCl-PEG (1:4) having the least intensity of OH peak around  $3401.80\text{ cm}^{-1}$ . The general trend for intensity of the OH peak of each type of DES mainly follows the trend of HBD which was mentioned earlier, and only a slight deviation of  $10\text{--}50\text{ cm}^{-1}$  is found. For ChCl-GLY (1:4) and ChCl-EG (1:4), the wavenumber shifted to the right compared to that of GLY and EG, while for ChCl-TEG (1:4) and ChCl-PEG (1:4), the wavenumber is found to shift to the left compared to that of TEG and PEG. The shifting of frequency numbers of OH peaks in DES might be due to the energy utilization for the formation of new bonds on the C-OH bonds in the HBD and also the hydrogen bonding formed between H-Cl as illustrated previously. Overall, ChCl-PEG (1:4) has the highest frequency of OH stretching vibration while ChCl-GLY (1:4) has the lowest frequency of OH stretching vibration in the spectra.

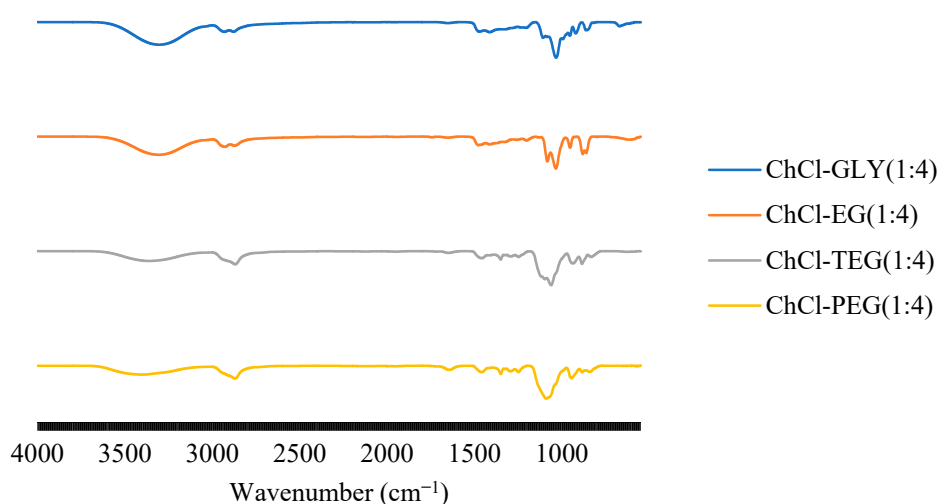


Figure 5. FTIR graph of DES with mole ratio of 1:4 hydrogen bond acceptor:hydrogen bond donor (HBA:HBD).

It was found that all the DESs and HBDs showed the C-H stretching vibration around frequency of  $2840\text{--}3000\text{ cm}^{-1}$ , where vibrations found around  $2950\text{--}2975\text{ cm}^{-1}$  and  $2865\text{--}2885\text{ cm}^{-1}$  are mostly contributed from the  $\text{CH}_3$  vibration, and stretching band produced by  $\text{CH}_2$  vibrations mainly occurred at  $2915\text{--}2940\text{ cm}^{-1}$  and  $2840\text{--}2875\text{ cm}^{-1}$  [33,34]. The DES have methyl group which are contributed

from the choline chloride having three free methyl groups, and also  $-\text{CH}_2$  group contributed from the respective HBD as most of their carbon center are linked to the oxygen atom. For instance, TEG and PEG obtain a single sharp peak at  $2868.75\text{ cm}^{-1}$  and  $2867.32\text{ cm}^{-1}$ , respectively, whereas their respective DES, namely ChCl-TEG (1:4) and ChCl-PEG (1:4) also producing one sharp peak around  $2869.56\text{ cm}^{-1}$  and  $2870.34\text{ cm}^{-1}$ . However, for GLY and EG, double peaks are seen at  $2937.83\text{ cm}^{-1}$  and  $2882.86\text{ cm}^{-1}$  for GLY, while  $2929.92\text{ cm}^{-1}$  and  $2875.00\text{ cm}^{-1}$  for EG; however, these two peaks are less intense compared to that of TEG and PEG. The similar double peaks are found for ChCl-GLY and ChCl-EG which occurs at  $2932.15\text{ cm}^{-1}$  and  $2877.00\text{ cm}^{-1}$  for ChCl-GLY, whereas  $2927.88\text{ cm}^{-1}$  and  $2873.72\text{ cm}^{-1}$  for the latter. However, none of the DES show similar peak found in ChCl around  $3024.67\text{ cm}^{-1}$ , contributed by the N-H stretching.

Another significant peak that can be used for comparison is the C-OH and C-O-C stretching vibration, which occur in every spectrum of the DESs, including single or double positive peaks around the wavenumbers of  $1033.33\text{--}1108.95\text{ cm}^{-1}$ . Overall, the C-OH and C-O-C stretching for DES is almost the same with a  $5\text{ cm}^{-1}$  difference in wavenumbers. This further concludes that the internal structure of HBD will remain the same in DES, the reaction between the choline chloride and the HBD only includes the formation of hydrogen bonding between terminal hydroxyl group from HBD and chloride ion from choline chloride salt.

Figure 6 shows the comparison of FTIR graph between ChCl-PEG (1:4) with its respective pure components. It is found that FTIR graph of ChCl-PEG (1:4) matches the FTIR graph of PEG rather than ChCl. In other words, the DES tends to share similar functional group with its HBD, rather than ChCl, which is their HBA. Observed in Figure 7, there is no difference in the FTIR graph among the ChCl-GLY with different mole ratio of HBA to HBD as they have the same functional group.

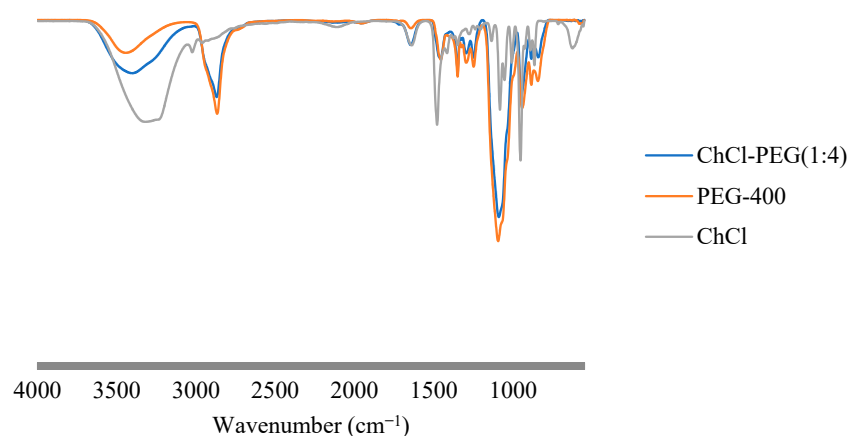


**Figure 6.** Comparison of ChCl-PEG (1:4) FTIR graph with its respective pure components.

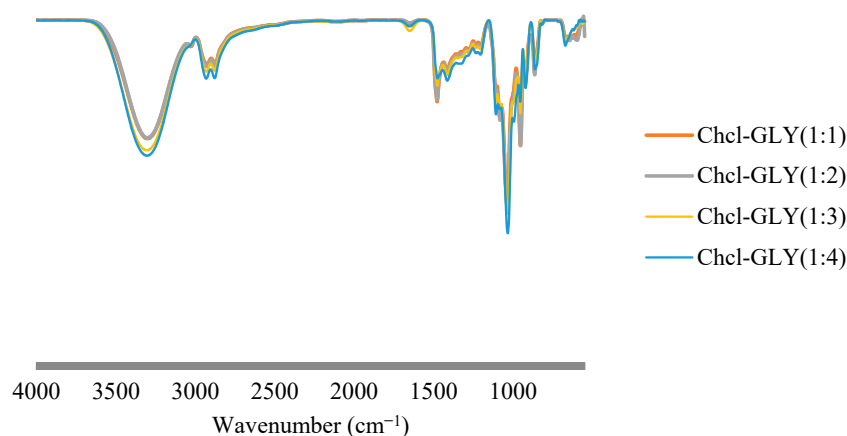


**Figure 7.** FTIR graph of ChCl-GLY with mole ratio of 1:1 to 1:4 (HBA:HBD).

### 3.4. Fuel Desulfurization Screening Results

The desulfurization performances of the DESs are compared in Figure 8. Only clear and transparent mixture without any insoluble precipitates, which is known as DES, was selected for the fuel desulfurization screening test as any insoluble precipitates present in the DES will hinder the DES from effectively removing SCC from the MO.

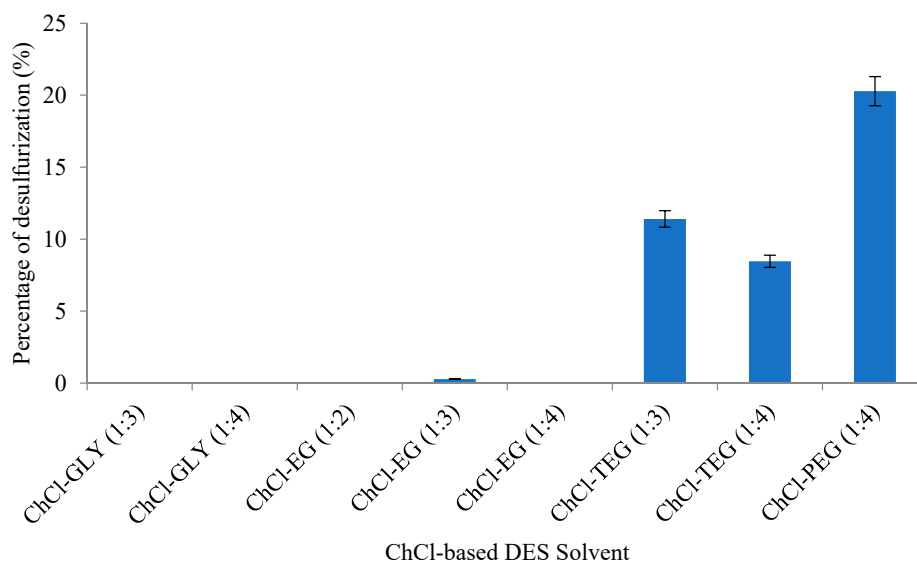


**Figure 8.** Desulfurization by selected DESs in model oil at 25 °C. The DES/ model oil (MO) ratio in the mixtures was 1:5, and the graphene oxide (GO) and H<sub>2</sub>O<sub>2</sub> dosages were 1:25 and 6:1, respectively.

According to the screening result presented in Figure 8, zero desulfurization percentage were found in four of the DESs, namely, ChCl-GLY(1:3), ChCl-GLY(1:4), ChCl-EG(1:2), and ChCl-EG (1:4). Although ChCl-EG (1:3) showed 0.28% desulfurization performance, it is too low to be considered in functioning as the desulfurizing agent. Hence, the author assumed that only ChCl-TEG and ChCl-PEG have the ability of removing SCC from the MO via ECODS method. The desulfurization performance increased in the order ChCl-TEG (1:4) < ChCl-TEG (1:3) < ChCl-PEG (1:4). The zero desulfurization percentage in both ChCl-GLY (1:3) and ChCl-GLY (1:4) might be due to the formation of extensive hydrogen bonding network within the ChCl-GLY DESs as it has high viscosity around 400–450 cP (Figure 3) at room temperature. The high viscosity value restricts the mobility of free species in ChCl-GLY; thus, ChCl-GLY failed to extract any SCC from the MO.

As for ChCl-EG, it is known that EG, which is the HBD component is very reactive and according to the thermogravimetric analysis by Degaldo and his colleague, ChCl-EG DES have relatively lower onset decomposition temperature (380–390 K) than other synthesized DES in their study. For instance, they found that ChCl-GLY has onset decomposition temperature range from 457 K to 500 K [35]. Low onset decomposition temperature suggests that ChCl-EG was relatively more unstable compared to other synthesized ChCl-based DESs in this study, which leads to undesired desulfurization result observed in the screening result.

The ChCl-PEG (1:4) has the highest desulfurization performance among all the ChCl-based DESs, removing 20.28% of SCC from the MO. Thus, ChCl-PEG (1:4) was selected to be further used in the optimization of the desulfurization parameters.

### 3.5. Optimization of the Desulfurization Parameters

#### 3.5.1. Volume Ratio of DES to the Model Oil

The ChCl-PEG (1:4) DES and the MO were mixed in six different volume ratios (Figure 9a), and the mixtures were stirred at 400 rpm for one hour at room temperature. Desulfurization improved as the

amount of DES in the MO increased. Mixtures with DES/MO volume ratios of 2.5:1 and 1:1 served as controls to assess the desulfurization capability of ChCl-PEG (1:4), and maximum desulfurization (82%) was achieved with a DES/MO volume ratio of 2.5:1. However, given the cost of DES production, achieving moderately good results with a smaller amount of DES is preferable to using such a large quantity. In a previous study, a large DES/MO volume ratio yielded only modest improvements in desulfurization performance [36]. The authors of the study reported that multistage extraction was more effective. However, increasing the DES/MO ratio has most often been found to improve desulfurization [11,37,38]. Satisfactory desulfurization (36.75%) was achieved at a DES/MO volume ratio of 1:2.5, and this DES/MO volume ratio was selected for following experiment.

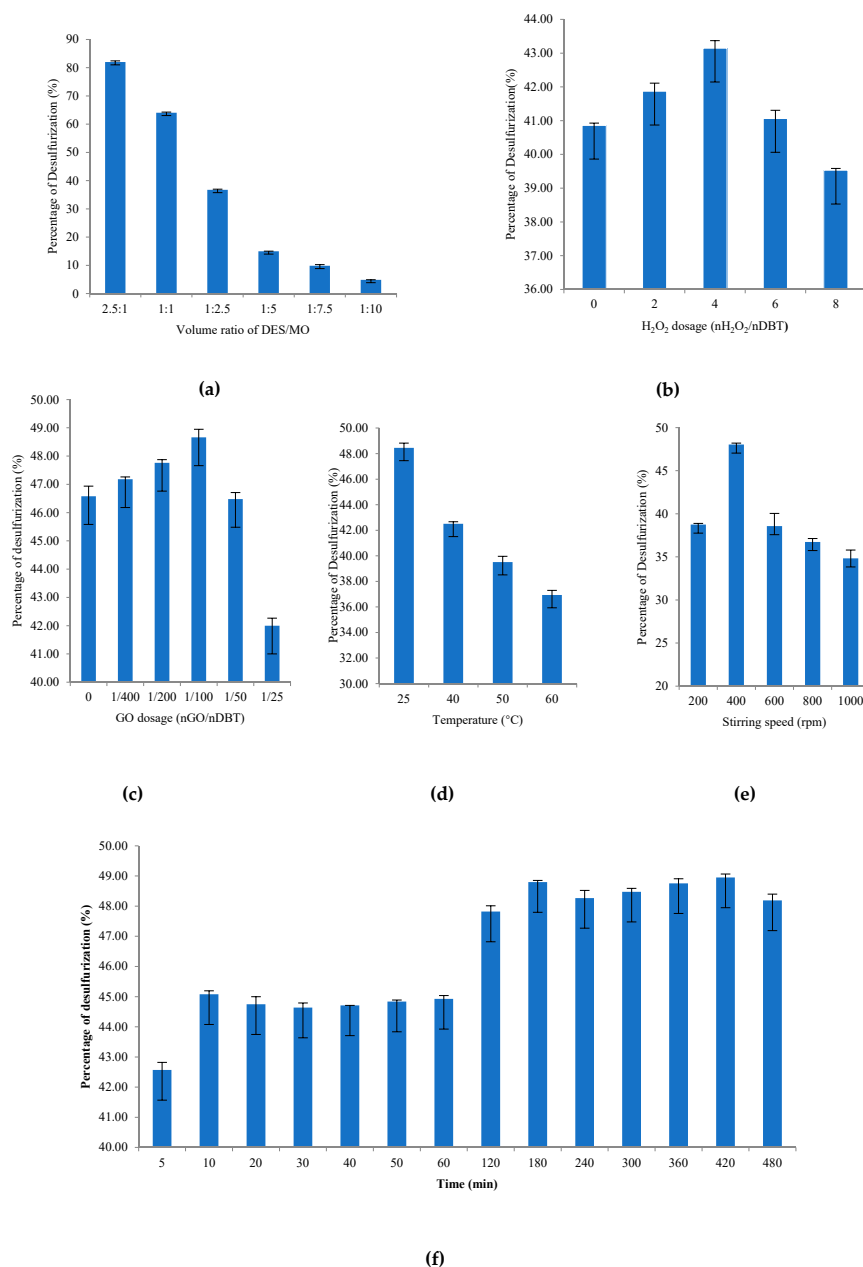


**Figure 9.** The optimized parameters of extractive catalytic oxidative desulfurization (ECODS) method including (a) DES/MO ratio (b) H<sub>2</sub>O<sub>2</sub>/s molar ratio (c) GO/S mass ratio (d) reaction temperature (e) stirring speed and (f) reaction time.

### 3.5.2. Effect of Oxidant Amount

Study was conducted for the effect of the oxidant dosage on the ECODS process by varying the molar ratio of H<sub>2</sub>O<sub>2</sub> to SCC. Desulfurization was performed at 25 °C for six hours using reaction mixtures with a GO/S mass ratio of 1:25. The stoichiometric reaction in Equation (1) shows that two moles of H<sub>2</sub>O<sub>2</sub> reacts with one mole of DBT to form a sulfone (DBTO<sub>2</sub>). Therefore, the molar ratio of H<sub>2</sub>O<sub>2</sub> to SCC was expected to have a significant impact on desulfurization. An H<sub>2</sub>O<sub>2</sub> dosage above two has been reported to improve desulfurization efficiency; however, excessive amount of oxidant will deplete the desulfurization efficiency, attributed by the non-productive thermal decomposition of the oxidant [20].



The extent of desulfurization increased incrementally from 40.86% to 41.87% when the H<sub>2</sub>O<sub>2</sub>/S molar ratio was increased from 0:1 to 1:25 and reached 43.15% when the H<sub>2</sub>O<sub>2</sub>/S molar ratio was increased to 4:1 (Figure 9b). This confirmed that the addition of H<sub>2</sub>O<sub>2</sub> enhanced the desulfurization. However, increasing the oxidant dosage further did not improve the desulfurization efficiency. Desulfurization decreased to 41.06% and 39.53% when the H<sub>2</sub>O<sub>2</sub>/S molar ratios were increased to 6:1 and 8:1, respectively, which was consistent with trends observed in previous studies [16,39]. Excessive amount of H<sub>2</sub>O<sub>2</sub> yields water as by-product. The water or moisture produced dilutes the reaction mixture, reducing the catalytic efficiency. We thus determined that the optimal H<sub>2</sub>O<sub>2</sub>/S molar ratio is 4:1.

### 3.5.3. Catalyst Dosage

The effect of varying the catalyst dosage on desulfurization by ChCl-PEG (1:4) was evaluated by preparing reaction mixtures with five different GO/S mass ratios and a H<sub>2</sub>O<sub>2</sub>/S molar ratio of 4:1. Desulfurization was then allowed to proceed for six hours at room temperature. The optimal GO/S ratio was found to be 1:100, with a removal of 48.66% (Figure 9c). Lower GO/S mass ratios of 1:400 and 1:200 demonstrated a reduction in the desulfurization with a removal of 47.18% and 47.76%, respectively. The extent of desulfurization was significantly lower in a mixture with higher GO/S mass ratio of 1:50 (46.48%) and GO/S mass ratio of 1:25 (42%). Interestingly, 46.6% desulfurization was achieved without the catalyst.

The unique layered structure of GO provides a large surface area, which promotes collisions between molecules. Increasing the GO/S ratio from 1:400 to 1:100 provided more surface area for molecules to bind, and desulfurization proceeded until the sites on the GO catalyst were saturated. GO/S ratios of 1:50 and 1:25 resulted in poorer desulfurization, because the excess GO allosterically hindered interactions between the catalyst and the substrate.

### 3.5.4. Effect of Temperature

The effect of the reaction temperature on desulfurization was also investigated. Desulfurization was performed for six hours at four different temperatures using mixtures with the optimized oxidant and catalyst dosages. Desulfurization by ChCl-PEG (1:4) decreased as the temperature increased. At reaction temperatures of 25 °C, 40 °C, 50 °C, and 60 °C, the desulfurization percentages were 48.45%, 42.51%, 39.51%, and 36.93%, respectively (Figure 9d). Similar results were obtained in previous studies, in which 25 °C was found to be the optimum temperature for IL and DES extraction [12,37,40,41]. Increasing the reaction temperature resulted in lower rates of desulfurization.

### 3.5.5. Effect of Stirring Speed

The optimal stirring speed for the ECODS process was found to be 400 rpm, with removal of 48% SCC using the ChCl-PEG (1:4) DES (Figure 9e). Desulfurization increased from 38.75 to 48.04% when the stirring speed was increased from 200 rpm to 400 rpm. This was due to the likelihood of collisions between the catalyst, the DES and DBT in the model oil being higher at 400 rpm. Increasing the number of collisions thus enabled the DES to remove more SCC. However, desulfurization decreased to 38.57%,

36.73% and 34.83% when the stirring speed was increased to 600, 800 and 1000 rpm, respectively. This may have been due to the limitations of the heating block since the optimal conditions could only be achieved at a stirring speed of 400 rpm.

### 3.5.6. Effect of Reaction Time

Desulfurization was performed using the ChCl-PEG (1:4) DES for a total of eight hours. MO samples were collected every five to ten minutes during the first hour. Samples were then collected hourly until eight hours passed. The results are shown in Figure 9f. The percentage of desulfurization increased slightly from 42.5 at minute five to 45% at minute ten and reached a plateau within the first hour. These results were consistent with those of previous studies. The optimal extraction time reported for DES extraction was 10 min, although desulfurization was monitored for only 60 min [11,38]. Increasing the reaction time to eight hours was done to determine whether desulfurization continued after the first 60 min. A slight increase from 45 to 47.8% was observed between hour one and hour two. The percentage increased to 48.8% by hour three, after which no additional desulfurization was observed. It was concluded that three hours was the optimal reaction time. However, to minimize energy consumption and control costs, subsequent reactions were allowed to proceed for 10 min.

### 3.6. Multistage Extraction

In multistage extraction, ChCl-PEG (1:4) DES was replaced with fresh ChCl-PEG (1:4) after each cycle. A mixture containing DES/MO ratio of 1:2.5, H<sub>2</sub>O<sub>2</sub>/S ratio of 6:1 and GO/S ratio of 1:100 was used for the first desulfurization cycle. The mixture was stirred for 10 min at room temperature. The same reaction condition was set as referred to previous desulfurization cycle and the steps were repeated for a total of six desulfurization cycles. The percentage of desulfurization increased from 49.65 in the first cycle to 95.68% in the sixth cycle (Figure 10). The S concentration in the oil was 4.72 ppm after the sixth desulfurization cycle, which satisfied the Euro 5 standard criterion (<10 ppm).

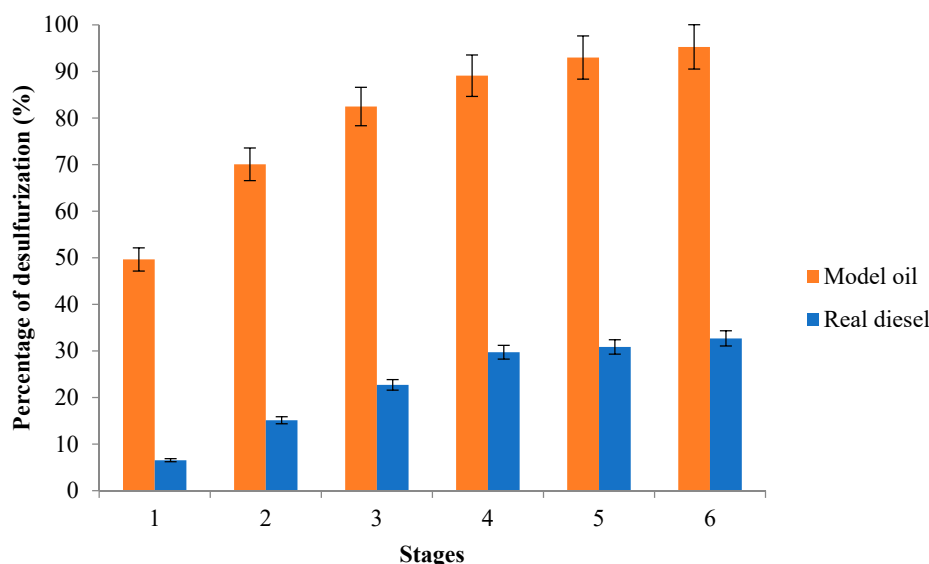


**Figure 10.** Desulfurization performance of ChCl-PEG (1:4) in 100 ppm model oil and real diesel fuel.

### 3.7. Desulfurization Performance in Real Diesel Fuel

The desulfurization performance of the ChCl-PEG (1:4) DES was then evaluated using real diesel fuel obtained from the Petronas fuel station. The desulfurization performance of ChCl-PEG (1:4) in 100 ppm MO and real diesel was compared as shown in Figure 10. It was expected that the ChCl-PEG (1:4) DES would be less effective in real diesel fuel, because it contained additional sulfur species and

impurities. Desulfurization of the diesel fuel and the 100 ppm MO followed similar trends throughout the six desulfurization cycles. However, desulfurization of the real diesel fuel reached a maximum of only 32.7%.

#### 4. Conclusions

ECODS method was utilized in this study, where  $H_2O_2$  was used as oxidant, and GO as catalyst to evaluate the fuel desulfurization performance of ChCl-based DES in 100 ppm model oil and also real diesel fuel. ChCl-PEG (1:4) was selected after the screening result as ChCl-PEG (1:4) successfully removed 20.28% SCC in MO, which is the highest desulfurization percentage among all the prepared ChCl-based DES. After rounds of experiment, the optimal reaction conditions for the ECODS method were found to be DES/MO volume ratio of 1:2.5, GO/S mass ratio of 1:100,  $H_2O_2$ /S molar ratio of 4:1, 10 min reaction time per cycle, stirring speed at 400 rpm and reaction temperature of 25 °C. Lastly, the desulfurization performance of ChCl-PEG(1:4) reached 32.7% in real diesel fuel and 95.28% in MO. Surprisingly, the addition of  $H_2O_2$  and GO only slightly increased the desulfurization performance of ChCl-PEG (1:4), which concludes that EDS method is good enough for the ChCl-PEG (1:4); however, this study demonstrated that ECODS method is fairly useful in increasing the desulfurization performance, however it is found not applicable commercially to the petroleum refinery industry. It is suggested that the EDS method is good enough for the DES in future work.

**Author Contributions:** Funding acquisition, H.F.M.Z.; investigation, C.Y.L.; project administration, H.F.M.Z.; supervision, H.F.M.Z., K.J. and F.K.C.; validation, M.F.M.; Writing—original draft, C.Y.L.; writing—review & editing, M.F.M. and S.R. All authors have read and agreed to the published version of the manuscript.

**Funding:** This research was funded by Yayasan UTP, grant number 015-LC017.

**Acknowledgments:** The authors would like to thank YUTP grant (015LC0-047) grant which supports the completion of this study. The authors would like to show appreciation to Universiti Teknologi Petronas and Centre of Research for Ionic Liquid (CORIL) for the opportunity and facilities provided throughout this work.

**Conflicts of Interest:** The authors declare no conflict of interest.

#### References

1. Ibrahim, M.H.; Hayyan, M.; Hashim, M.A.; Hayyan, A. The role of ionic liquids in desulfurization of fuels: A review. *Renew. Sustain. Energy Rev.* **2017**, *76*, 1534–1549. [[CrossRef](#)]
2. Bradford, M.A.; Wookey, P.A.; Ineson, P.; Lappin-Scott, H.M. Controlling factors and effects of chronic nitrogen and sulphur deposition on methane oxidation in a temperate forest soil. *Soil Biol. Biochem.* **2001**, *33*, 93–102. [[CrossRef](#)]
3. Silitonga, A.S.; Atabani, A.E.; Mahlia, T.M.I. Review on fuel economy standard and label for vehicle in selected ASEAN countries. *Renew. Sustain. Energy Rev.* **2012**, *16*, 1683–1695. [[CrossRef](#)]
4. Mahlia, T.M.I.; Saidur, R.; Memon, L.A.; Zulkifli, N.W.M.; Masjuki, H.H. A review on fuel economy standard for motor vehicles with the implementation possibilities in Malaysia. *Renew. Sustain. Energy Rev.* **2010**, *14*, 3092–3099. [[CrossRef](#)]
5. Majid, M.F.; Mohd Zaid, H.F.; Kait, C.F.; Jumbri, K.; Yuan, L.C.; Rajasuriyan, S. Futuristic advance and perspective of deep eutectic solvent for extractive desulfurization of fuel oil: A review. *J. Mol. Liq.* **2020**, *306*, 112870. [[CrossRef](#)]
6. Soleimani, M.; Bassi, A.; Margaritis, A. Biodesulfurization of refractory organic sulfur compounds in fossil fuels. *Biotechnol. Adv.* **2007**, *25*, 570–596. [[CrossRef](#)]
7. Bandyopadhyay, S.; Chowdhury, R.; Bhattacharjee, C.; Pan, S. Simultaneous production of biosurfactant and ULSD (ultra low sulfur diesel) using *Rhodococcus* sp. in a chemostat. *Fuel* **2013**, *113*, 107–112. [[CrossRef](#)]
8. Bandyopadhyay, S.; Chowdhury, R.; Bhattacharjee, C. Mathematical modeling of production of bio-surfactant through bio-desulfurization of hydrotreated diesel in a fermenter. *AIP* **2010**, *1298*, 232–237.
9. Ju, F.; Wang, M.; Wu, T.; Ling, H. The role of NiO in reactive adsorption desulfurization over NiO/ZnO-Al<sub>2</sub>O<sub>3</sub>-SiO<sub>2</sub> adsorbent. *Catalysts* **2019**, *9*, 79. [[CrossRef](#)]



10. Zheng, M.; Hu, H.; Ye, Z.; Huang, Q.; Chen, X. Adsorption desulfurization performance and adsorption-diffusion study of B<sub>2</sub>O<sub>3</sub> modified Ag-CeO<sub>x</sub>/TiO<sub>2</sub>/SiO<sub>2</sub>. *J. Hazard. Mater.* **2019**, *362*, 424–435. [[CrossRef](#)]
11. Mohd Zaid, H.F.; Chong, F.K.; Abdul Mutalib, M.I. Extractive deep desulfurization of diesel using choline chloride-glycerol eutectic-based ionic liquid as a green solvent. *Fuel* **2017**, *192*, 10–17. [[CrossRef](#)]
12. Gano, Z.S.; Mjalli, F.S.; Al-Wahaibi, T.; Al-Wahaibi, Y.; AlNashef, I.M. Extractive desulfurization of liquid fuel with FeCl<sub>3</sub> based deep eutectic solvents: Experimental design and optimization by central-composite design. *Chem. Eng. Process. Process Intensif.* **2015**, *93*, 10–20. [[CrossRef](#)]
13. Betiha, M.A.; Rabie, A.M.; Ahmed, H.S.; Abdelrahman, A.A.; El-Shahat, M.F. Oxidative desulfurization using graphene and its composites for fuel containing thiophene and its derivatives: An update review. *Egypt. J. Pet.* **2018**, *27*, 715–730. [[CrossRef](#)]
14. Andevary, H.H.; Akbari, A.; Omidkhan, M. High efficient and selective oxidative desulfurization of diesel fuel using dual-function [Omim] FeCl<sub>3</sub> as catalyst/extractant. *Fuel Process. Technol.* **2019**, *185*, 8–17. [[CrossRef](#)]
15. Rezvani, M.A.; Shaterian, M.; Aghmasheh, M. Catalytic oxidative desulphurization of gasoline using amphiphilic polyoxometalate polymer nanocomposite as an efficient, reusable, and green organic-inorganic hybrid catalyst. *Environ. Technol.* **2020**, *41*, 1219–1231. [[CrossRef](#)] [[PubMed](#)]
16. Lü, H.; Li, P.; Liu, Y.; Hao, L.; Ren, W.; Zhu, W.; Deng, C.; Yang, F. Synthesis of a hybrid Anderson-type polyoxometalate in deep eutectic solvents (DESs) for deep desulphurization of model diesel in ionic liquids (ILs). *Chem. Eng. J.* **2017**, *313*, 1004–1009. [[CrossRef](#)]
17. Julião, D.; Gomes, A.C.; Pillinger, M.; Lopes, A.D.; Valença, R.; Ribeiro, J.C.; Gonçalves, I.S.; Balula, S.S. Desulfurization of diesel by extraction coupled with Mo-catalyzed sulfoxidation in polyethylene glycol-based deep eutectic solvents. *J. Mol. Liq.* **2020**, *309*, 113093. [[CrossRef](#)]
18. Görmez, F.; Görmez, Ö.; Gözmen, B.; Kalderis, D. Degradation of chloramphenicol and metronidazole by electro-Fenton process using graphene oxide-Fe<sub>3</sub>O<sub>4</sub> as heterogeneous catalyst. *J. Environ. Chem. Eng.* **2019**, *7*, 102990. [[CrossRef](#)]
19. Rezvani, M.A.; Shokri Aghbolagh, Z.; Hosseini Monfared, H.; Khandan, S. Mono Mn(II)-substituted phosphotungstate modified graphene oxide as a high-performance nanocatalyst for oxidative demercaptanization of gasoline. *J. Ind. Eng. Chem.* **2017**, *52*, 42–50. [[CrossRef](#)]
20. Chandran, D.; Khalid, M.; Walvekar, R.; Mubarak, N.M.; Dharaskar, S.; Wong, W.Y.; Gupta, T.C.S.M. Deep eutectic solvents for extraction-desulphurization: A review. *J. Mol. Liq.* **2019**, *275*, 312–322. [[CrossRef](#)]
21. Smith, E.L.; Abbott, A.P.; Ryder, K.S. Deep Eutectic Solvents (DESs) and Their Applications. *Chem. Rev.* **2014**, *114*, 11060–11082. [[CrossRef](#)] [[PubMed](#)]
22. Jangir, A.K.; Patel, D.; More, R.; Parmar, A.; Kuperkar, K. New insight into experimental and computational studies of Choline chloride-based ‘green’ ternary deep eutectic solvent (TDES). *J. Mol. Struct.* **2019**, *1181*, 295–299. [[CrossRef](#)]
23. Liu, X.; Xu, D.; Diao, B.; Zhang, L.; Gao, J.; Liu, D.; Wang, Y. Choline chloride based deep eutectic solvents selection and liquid-liquid equilibrium for separation of dimethyl carbonate and ethanol. *J. Mol. Liq.* **2019**, *275*, 347–353. [[CrossRef](#)]
24. Wen, Q.; Chen, J.X.; Tang, Y.L.; Wang, J.; Yang, Z. Assessing the toxicity and biodegradability of deep eutectic solvents. *Chemosphere* **2015**, *132*, 63–69. [[CrossRef](#)]
25. Mbous, Y.P.; Hayyan, M.; Hayyan, A.; Wong, W.F.; Hashim, M.A.; Looi, C.Y. Applications of deep eutectic solvents in biotechnology and bioengineering—Promises and challenges. *Biotechnol. Adv.* **2017**, *35*, 105–134. [[CrossRef](#)] [[PubMed](#)]
26. Abo-Hamad, A.; Hayyan, M.; AlSaadi, M.A.H.; Hashim, M.A. Potential applications of deep eutectic solvents in nanotechnology. *Chem. Eng. J.* **2015**, *273*, 551–567. [[CrossRef](#)]
27. Lima, F.; Gouvenaux, J.; Branco, L.C.; Silvestre, A.J.D.; Marrucho, I.M. Towards a sulfur clean fuel: Deep extraction of thiophene and dibenzothiophene using polyethylene glycol-based deep eutectic solvents. *Fuel* **2018**, *234*, 414–421. [[CrossRef](#)]
28. Stefanovic, R.; Webber, G.B.; Page, A.J. Polymer solvation in choline chloride deep eutectic solvents modulated by the hydrogen bond donor. *J. Mol. Liq.* **2019**, *279*, 584–593. [[CrossRef](#)]
29. Makoś, P.; Boczkaj, G. Deep eutectic solvents based highly efficient extractive desulfurization of fuels—Eco-friendly approach. *J. Mol. Liq.* **2019**, *296*, 111916. [[CrossRef](#)]

30. Singh, S.K.; Savoy, A.W. Ionic liquids synthesis and applications: An overview. *J. Mol. Liq.* **2020**, *297*, 112038. [[CrossRef](#)]
31. Zainal-Abidin, M.H.; Hayyan, M.; Hayyan, A.; Jayakumar, N.S. New horizons in the extraction of bioactive compounds using deep eutectic solvents: A review. *Anal. Chim. Acta* **2017**, *979*, 1–23. [[CrossRef](#)] [[PubMed](#)]
32. Ghaedi, H.; Ayoub, M.; Sufian, S.; Lal, B.; Uemura, Y. Thermal stability and FT-IR analysis of Phosphonium-based deep eutectic solvents with different hydrogen bond donors. *J. Mol. Liq.* **2017**, *242*, 395–403. [[CrossRef](#)]
33. Socrates, G. Infrared and Raman characteristic group frequencies. Tables and charts. *J. Raman Spectrosc.* **2004**, *35*, 905.
34. Larkin, P. *Infrared and Raman Spectroscopy; Principles and Spectral Interpretation*; Elsevier: Amsterdam, The Netherlands, 2011; ISBN 9780123869845.
35. Delgado-Mellado, N.; Larriba, M.; Navarro, P.; Rigual, V.; Ayuso, M.; García, J.; Rodríguez, F. Thermal stability of choline chloride deep eutectic solvents by TGA/FTIR-ATR analysis. *J. Mol. Liq.* **2018**, *260*, 37–43. [[CrossRef](#)]
36. Wilfred, C.D.; Kiat, C.F.; Man, Z.; Bustam, M.A.; Mutalib, M.I.M.; Phak, C.Z. Extraction of dibenzothiophene from dodecane using ionic liquids. *Fuel Process. Technol.* **2012**, *93*, 85–89. [[CrossRef](#)]
37. Mokhtar, W.N.A.W.; Bakar, W.A.W.A.; Ali, R.; Kadir, A.A.A. Deep desulfurization of model diesel by extraction with N,N-dimethylformamide: Optimization by Box–Behnken design. *J. Taiwan Inst. Chem. Eng.* **2014**, *45*, 1542–1548. [[CrossRef](#)]
38. Khezeli, T.; Daneshfar, A. Synthesis and application of magnetic deep eutectic solvents: Novel solvents for ultrasound assisted liquid-liquid microextraction of thiophene. *Ultrason. Sonochem.* **2017**, *38*, 590–597. [[CrossRef](#)]
39. Mao, C.; Zhao, R.; Li, X. Phenylpropanoic acid-based DESs as efficient extractants and catalysts for the removal of sulfur compounds from oil. *Fuel* **2017**, *189*, 400–407. [[CrossRef](#)]
40. Li, Z.; Cui, Y.; Li, C.; Shen, Y. Deep desulfurization of fuels based on deep eutectic theory. *Sep. Purif. Technol.* **2019**, *219*, 9–15. [[CrossRef](#)]
41. Ahmed Rahma, W.S.; Mjalli, F.S.; Al-Wahaibi, T.; Al-Hashmi, A.A. Polymeric-based deep eutectic solvents for effective extractive desulfurization of liquid fuel at ambient conditions. *Chem. Eng. Res. Des.* **2017**, *120*, 271–283. [[CrossRef](#)]

**Publisher’s Note:** MDPI stays neutral with regard to jurisdictional claims in published maps and institutional affiliations.



© 2020 by the authors. Licensee MDPI, Basel, Switzerland. This article is an open access article distributed under the terms and conditions of the Creative Commons Attribution (CC BY) license (<http://creativecommons.org/licenses/by/4.0/>).